Food Chemistry: X 25 (2025) 102078

Contents lists available at ScienceDirect

Food Chemistry: X

journal homepage: www.sciencedirect.com/journal/food-chemistry-x

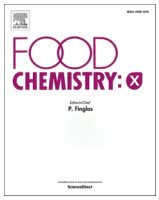

Antibacterial mechanism of *Lactiplantibacillus plantarum* SHY96 cell-free supernatant against *Listeria monocytogenes* revealed by metabolomics and potential application on chicken breast meat preservation

Ming Liang [a,b,1], Hongwei Wang [a,b,1], Zhaoquan Zhou [a,b], Yechuan Huang [c,*], Huayi Suo [a,b,**]

[a] College of Food Science, Southwest University, Chongqing 400715, China
[b] Chongqing Agricultural Product Processing Technology Innovation Platform, SouthwestUniversity, Chongqing 400715, China
[c] College of Bioengineering, Jingchu University of Technology, Jingmen 448000, China

ARTICLE INFO

Keywords:
Cell-free supernatants
Lactiplantibacillus plantarum
Listeria monocytogenes
Metabolomics
Meat product

ABSTRACT

The cell-free supernatant of *Lactiplantibacillus plantarum* (LCFS) is considered a potential natural antimicrobial agent due to its outstanding antimicrobial activity. This study demonstrated that the cell-free supernatant of *L. plantarum* SHY96 (LCFS96) effectively inhibits the growth and biofilm formation of *L. monocytogenes* CMCC(B) 54002 (*L. monocytogenes*_02) by reducing cell metabolic activity and damaging cell structure. Metabolomic analysis revealed that LCFS96 significantly altered 450 intracellular metabolites, affecting key metabolic pathways including linoleic acid metabolism, pyrimidine metabolism, purine metabolism, pantothenic acid and CoA biosynthesis, and the TCA cycle. Additionally, application of LCFS96 significantly reduced *L. monocytogenes*_02 viable counts by 84.93%, while maintaining the pH, TVB-N and organoleptic properties of chicken meat under refrigeration at 4 °C for 12 days. These findings highlight the antimicrobial mechanism and potential application of LCFS96 in extending the shelf-life of meat products.

1. Introduction

Foodborne pathogens pose a significant challenge to food safety in manufacturing and constitute a significant threat to human health (Khan et al., 2023). *Listeria monocytogenes* is among the most important foodborne pathogens, being prevalent worldwide and commonly associated with several foodborne outbreaks (Bodie et al., 2023). Recent epidemiological data from the World Health Organization have indicated a high mortality rate among people infected with *L. monocytogenes* globally (FAO and WHO, 2022). In 2020, a 22% mortality rate was observed in the United States among individuals infected with *L. monocytogenes*. In addition, the European Food Safety Agency (EFSA) reported 183 cases of *L. monocytogenes* in the EU in 2021 (European Food Safety Authority and European Centre for Disease Prevention and Control, 2022). Consequently, the widespread dissemination and significant health risks associated with *L. monocytogenes* have escalated into a major public health concern.

L. monocytogenes infections are associated with a variety of food sources, with meat products being a significant source of contamination (Liu, Liu, et al., 2020). Meat, rich in protein, fat, and other essential nutrients, provides an ideal environment for the growth and proliferation of *L. monocytogenes* (Jamshidi & Zeinali, 2019). *L. monocytogenes* is particularly significant for its ability to form biofilms and endure a range of environmental conditions, such as high salt concentrations, low temperatures, low pH, and low humidity (He et al., 2023). Thus, meat products are at risk of contamination with *L. monocytogenes* throughout all phases of production, including manufacturing, processing, distribution, and even after cooking (Marmion et al., 2022).

To date, the primary strategy for preventing *L. monocytogenes* contamination in the food industry involves rigorous hygiene maintenance during meat processing (Palma et al., 2020). However, the effective control of meat contamination still constitutes a considerable challenge for the industry. In recent years, an increasing demand for natural preservative technology without side effects to enhance food

* Corresponding author.
** Corresponding author at: College of Food Science, Southwest University, Chongqing 400715, China.
E-mail addresses: hyc2005@sina.com (Y. Huang), birget@swu.edu.cn (H. Suo).
[1] The first two authors contributed equally to this paper.

https://doi.org/10.1016/j.fochx.2024.102078
Received 18 July 2024; Received in revised form 27 November 2024; Accepted 8 December 2024
Available online 9 December 2024

preservation and reduce microbial contamination has been observed among consumers. Recent studies have shown that deep learning-based systems have the potential to optimize food packaging, thus indirectly contributing to the preservation of product quality and safety (Zhang, Chen, et al., 2023). In addition, innovative packaging systems, such as fuzzy PID-based gas dispensing, can create optimal environments that prevent microbial growth, extend shelf life, and complement the role of natural preservatives (Zhang, Zuo, et al., 2023). These advances highlight the importance of an integrated approach that utilizes novel packaging technologies and preservatives to address the challenges of microbial contamination in food. Therefore, there is an urgent need for the development and industrial application of novel natural preservative methods specifically targeting *L. monocytogenes* in meat products.

Probiotics and their metabolites are considered ideal biopreservatives owing to their health-associated benefits, safety, environmental friendliness, readiness, and strong antimicrobial properties (Silva et al., 2020). In particular, lactic acid bacteria (LAB) have shown excellent antimicrobial effects against several foodborne pathogens. For instance, LAB strains (J.27 and M.21) isolated from Korean kimchi have shown excellent anti-biofilm activity against foodborne pathogens such as *Vibrio parahaemolyticus*, *Pseudomonas aeruginosa*, and *Escherichia coli*. Moreover, these two LAB strains have been shown to effectively inhibit biofilm formation on surfaces in contact with seafood, such as squid (Toushik et al., 2021). Moreover, cell-free supernatants from LAB isolated from fermented beverages and fish have demonstrated antibacterial activity against a wide range of Gram-positive and Gram-negative foodborne bacteria (Dejene et al., 2021). Notably, *Lactiplantibacillus plantarum* cell-free supernatant (LCFS) has shown an excellent safety profile and is less likely to contribute to the emergence of microbial tolerance and/or resistance (Yilmaz et al., 2022). However, to the best of our knowledge, studies on the activity of LCFS against *L. monocytogenes*, especially regarding its mechanism of action, are still lacking.

Metabolomics has been widely used to explore dynamic changes in bacteria at the metabolic level, having become an effective tool to study antibacterial mechanisms (Zhao et al., 2021). For instance, using metabolomics analysis, He et al. (2022) found that linalool inhibits the growth of *L. monocytogenes* by interfering with metabolic pathways involved in amino acid metabolism, central carbon metabolism, lipid metabolism, and nucleic acid metabolism, while 2-methoxycinnamaldehyde was found to inhibit the growth of methicillin-resistant *Staphylococcus epidermidis* by interfering with the TCA cycle and the pentose phosphate pathway (Qian et al., 2022). Therefore, metabolomics can be considered a promising strategy to study the antibacterial mechanism of LCFS against *L. monocytogenes*.

In the light of this, the aim of the present study was to apply untargeted metabolomics to investigate the antibacterial mechanism of LCFS on *L. monocytogenes*. Moreover, the application potential of LCFS to chicken breast meat was evaluated. The findings discussed herein contribute to the application of LCFS as a natural preservative in meat products.

2. Materials and methods

2.1. Bacterial strains

L. plantarum SHY96, isolated from traditional Sichuan kimchi in China, is deposited at the China Center for Type Culture Collection under the collection number CCTCC M 2024399. This strain was identified through Gram staining and 16S rDNA sequencing, along with evolutionary tree analysis, as illustrated in Fig. S1. It was pre-cultured in de Man Rogosa Sharpe (MRS) broth (Land Bridge Technology Co., Ltd., Beijing, China) at 37 °C for 24 h. Preliminary antibacterial screening of 50 strains of food-associated lactic acid bacteria from laboratory culture collection revealed that *L. plantarum* SHY96 exhibits potent antimicrobial activity against pathogenic microorganisms such as *L. monocytogenes*.

L. monocytogenes CMCC(B)54002 (*L. monocytogenes*_02) was purchased from the National Center for Medical Culture Collections (CMCC, No54002). This strain was widely studied and serves as a model pathogen for evaluating the antimicrobial properties of probiotics and lactic acid bacteria. It was cultured at 37 °C for 24 h in tryptone soybean broth (TSB) (Hope Bio-Technology Co., Ltd., Qingdao, China).

2.2. Preparation and concentration of CFS of L. plantarum

Preparation and concentration of *L. plantarum* SHY96 cell-free supernatant (LCFS96) was performed following a method previously described by Xu et al. (2024). Briefly, *L. plantarum* SHY96 was cultured in 300 mL MRS broth and incubated at 37 °C for 24 h. After incubation, the suspension (10^9 CFU/mL) was submitted to centrifugation at 6,000 rpm for 10 min at 4 °C to collect the cell-free supernatant. Subsequently, the supernatant was concentrated in a rotary evaporator and then submitted to lyophilization in a lyophilizer (Songyuan Huaxing Technology Develop Co., Ltd., Beijing, China). The resulting powder, i.e., LCFS96, was accurately weighed in an analytical balance and then dissolved in sterile water to prepare a solution at a final concentration of 200 mg/mL. Dissolved CFS samples were stored at −80 °C until subsequent analysis, and sterile MRS was used as background control.

2.3. Determination of the antibacterial activity of LCFS96

2.3.1. Determination of the minimum inhibitory concentration (MIC)

MIC values of LCFS96 against *L. monocytogenes*_02 were determined using the broth microdilution assay, as previously described (Jiang et al., 2022). Briefly, 180 μL of TSB containing *L. monocytogenes*_02 planktonic cells (10^6 CFU/mL) was mixed with 20 μL of LCFS96 to obtain solutions at different final concentrations, i.e., 0.625, 1.25, 2.5, 5, 10, and 20 mg/mL, respectively. Subsequently, the solution was placed in a 96-well plate and incubated at 37 °C for 24 h. The growth of *L. monocytogenes*_02 planktonic cells was assessed by measuring the absorbance of the suspensions at 600 nm (OD_{600}) in a microplate reader (Gen5TM, BioTek® Instruments, Inc., Winooski, USA). The MIC value was defined as the lowest concentration of LCFS96 that resulted in no visible growth of *L. monocytogenes*_02. Cells without the addition of LCFS96 were considered as the control sample.

2.3.2. Growth curve and time-kill kinetics assays

The inhibitory effect of LCFS96 against *L. monocytogenes*_02 was investigated by constructing growth curves (Ma et al., 2023). Briefly, LCFS96 was added to *L. monocytogenes*_02 planktonic cells (10^6 CFU/mL) to obtain different final concentrations based on the MIC value, i.e., 1/2× MIC, 1× MIC, and 2× MIC. After homogenization, bacterial suspensions were incubated at 37 °C for 24 h, during which time the absorbance (OD_{600}) was determined hourly. Cells without the addition of LCFS96 served as the control sample.

Time-kill kinetics assays were conducted to determine the killing effects of LCFS96 on *L. monocytogenes*_02 planktonic cells over a three-hour period, as previously described (Ma et al., 2023). LCFS96 was added to *L. monocytogenes*_02 planktonic cells (10^6 CFU/mL) to obtain mixtures at different final concentrations based on the MIC value, i.e., 1/2× MIC, 1× MIC, and 2× MIC, followed by incubation at 37 °C for 0, 1, 2, and 3 h, respectively. Subsequently, 10 μL of the suspension from each incubation time point was coated on Tryptone Soy Agar (TSA) plates (Hope Bio-Technology Co., Ltd., Qingdao, China) after ten-fold serial dilution. After incubation at 37 °C for 48 h, colonies formed on plates were enumerated. Cells without the addition of LCFS96 served as the control sample.

2.3.3. Determination of the anti-biofilm activity

The inhibitory effect of LCFS96 on the capacity of *L. monocytogenes* to form biofilms was assessed based on previously described protocols (Luo et al., 2021). Briefly, 100 μL of *L. monocytogenes*_02 planktonic cells was

transferred to a 96-well plate, and an equal volume of LCFS96 was added to the wells to reach a final concentration of 1× MIC and 2× MIC. Following the incubation period, non-adhered bacterial cells were carefully discarded, and the wells were gently washed twice with PBS. Obtained *L. monocytogenes*_02 biofilms were then stained using the MycoLight™ Live Bacterial Fluorescence Imaging Kit (AAT Bioquest, Sunnyvale, CA, USA) and visualized under a fluorescence microscope (Bosda, Bosda, Shenzhen, China) at 100× magnification (excitation/emission: 500/550 nm). Mean fluorescence intensities were analyzed using ImageJ software version 1.54f (Wayne Rasband, National Institutes of Health, USA). Cells without the addition of LCFS96 served as the control sample.

2.4. Determination of the mechanism underlying the antimicrobial activity of LCFS96 against L. monocytogenes

2.4.1. Analysis of cell metabolic activity

The metabolic activity of *L. monocytogenes*_02 planktonic cells treated with LCFS96 was evaluated following established protocols (Jiang, Xin, Zhang, et al., 2022). Briefly, *L. monocytogenes*_02 cells (10^8 CFU/mL) were treated with LCFS96 at final concentrations of 1× MIC and 2× MIC, and incubated at 37 °C for 30 min. Following incubation time, *L. monocytogenes*_02 cells were centrifuged at 6,000 rpm for 5 min at 4 °C and then resuspended in PBS. Subsequently, a mixture of fluorescent dyes NucView Green and propidium iodide (PI) (3.0 μL per well) was added to bacterial cells followed by incubation in dark conditions for 30 min. Cells were then observed in a fluorescence microscope (Ex/Em: NucView Green: 500/530 nm; PI: 535/617 nm, 200× magnification). Control samples without LCFS96 treatment were also included in this experiment.

To further elucidate the effects of LCFS96 on the metabolic activity of *L. monocytogenes*_02 planktonic cells, the propidium iodide (PI) uptake assay was performed in a flow cytometer, as previously described (Jiang, Xin, Yang, et al., 2022). Briefly, *L. monocytogenes*_02 planktonic cells were cultured until the exponential phase was reached. Bacterial cells were collected by centrifugation at 6,000 rpm for 5 min at 4 °C and then resuspended in PBS to obtain a concentration of approximately 10^6 CFU/mL. Subsequently, LCFS96 was added to the bacterial suspensions to achieve a final concentration of 1× MIC and 2× MIC, and then incubated at 37 °C for 30 min. Subsequently, the PI solution (10 μg/mL) was added to the bacterial suspensions followed by incubation at 37 °C for 30 min in the dark. PI uptake was determined in a FACScan™ flow cytometer (Becton Dickinson, New Jersey, USA) with data analysis conducted using the WinMDI software v.2.9 (Scripps Research Institute, CA, USA). Samples without the addition of LCFS96 served as the control.

2.4.2. Scanning electron microscopy (SEM) analysis

Morphological changes in *L. monocytogenes*_02 planktonic cells treated with LCFS96 were evaluated using SEM, as previously described (Jiang et al., 2022) Initially, 1 mL of *L. monocytogenes*_02 cells (10^7 CFU/mL) were collected by centrifugation at 6,000 rpm for 5 min at 4 °C, followed by three washes with PBS. *L. monocytogenes*_02 cells were treated with LCFS96 at 1× MIC and 2× MIC and then incubated at 37 °C for 2 h. Subsequently, *L. monocytogenes*_02 cells were centrifuged again at 6,000 rpm for 5 min at 4 °C, washed three times with PBS, and then fixed in 2.5% glutaraldehyde at 4 °C for 8 h. Fixed cells were dehydrated using increasing concentrations of ethanol solution (i.e., 30%, 50%, 70%, 80%, and 95%) for 30 min in each concentration. Dehydrated cells were then dried, sputter-coated with gold, and examined in a Hitachi S-3000N SEM (Hitachi, Tokyo, Japan). Samples without LCFS96 served as the control.

2.5. Non-targeted metabolomics analysis

The non-targeted metabolomics analysis was evaluated following established protocols (Qian et al., 2022). *L. monocytogenes*_02 planktonic cells in logarithmic phase were treated with 1× MIC concentration of LCFS96 for 2 h, then centrifuged at 3,000 rpm at 4 °C for 10 min, followed by washing three times with PBS. The precipitate with bacterial cells (30 ± 5 mg) was obtained and resuspended in 300 μL of 80% methanol, ground for 6 min with a frozen tissue grinder, and submitted to cryosonication for 30 min at 5 °C to extract metabolites. After standing at −20 °C for 30 min, samples were centrifuged at 6,000 rpm at 4 °C for 15 min, and the supernatant was collected for UPLC-MS/MS analysis. Samples not treated with LCFS96 were analyzed in identical manner as samples treated with LCFS96. Each sample was analyzed as six independent replicates. During measurements, a QC sample was inserted every eight test samples in parallel to ensure quality control of the analytical process.

Raw LC-MS/MS data was imported into Progenesis QI software (Waters Co., Ltd., Massachusetts, Milford, USA) for analysis. Metabolites were identified using the Metabolism Public Database (HMDB) (http://www.hmdb.ca/), Metlin (https://metlin.scripps.edu/) and in-house Majorbio databases. The processed data matrix was uploaded to the Majorbio cloud platform (https://cloud.majorbio.com) for bioinformatic analysis. The metabolites satisfying variable importance in prediction (VIP) > 1, adjusted $P < 0.05$, and absolute fold change (FC) > 1 were defined as differentially accumulated metabolites (DAMs). Metabolic pathway annotation was performed using the KEGG database (http://www.genome.jp/kegg/). Pathway enrichment analyses were performed using the Python package scipy.stats (https://docs.scipy.org/doc/scipy/). Sample correlation analysis and principal component analysis (PCA) were performed using the ropls R package (version 1.6.2).

2.6. Application of LCFS96 to a chicken breast model

2.6.1. Chicken breast sample preparation

Chicken breast samples were prepared according to a previously described method with a few modifications (Ying et al., 2023). Chicken breasts were sourced from a local market (Chongqing, China) and transported to the laboratory at 4 °C. Chicken breasts were rinsed three times with sterile PBS at room temperature (25 °C) and cut into small pieces of approximately 1 cm × 1 cm × 2 cm, each weighing approximately 2 g. Chicken breast cuts were submitted to air-drying at room temperature until visually dry. Subsequently, meat samples were immersed for 15 min in LCFS96 solution at different concentrations, i.e., 0× MIC (Control), 1× MIC, and 2× MIC, followed by air-drying at room temperature. Then, 1 mL of *L. monocytogenes* suspension (10^5 CFU/mL) was inoculated using a sterile spray bottle on meat samples, followed by air-drying in aseptic conditions for 1 h. Finally, inoculated meat pieces were stored at 4 °C for 12 days, and removed for analysis on day 0, 2, 4, 6, 8, 10, and 12.

2.6.2. Microbiological analysis

The microbiological analysis was assessed based on previously described protocols (Xin et al., 2023). Briefly, 2 g of the treated meat sample was aseptically placed in a sterile bag containing 10 mL of 0.9% sterile saline. The mixture was homogenized at 6,000 rpm for 10 min using a BILON-08 homogenizer (Bilon Instrument Co., Ltd., Shanghai, China). Subsequently, 10 μL of the mixture was coated on TSA plates after a ten-fold serial dilution (Jiang, Xin, Yang, et al., 2022). After incubation at 37 °C for 48 h, colonies formed on plates were enumerated.

2.6.3. pH measurements

The pH of samples was determined based on the method GB 5009.237–2016 'National Standard for Food Safety Determination of pH Value of Food' with slight modifications (Yuan et al., 2021). Briefly, 2 g of the treated meat sample was added to 20 mL of saline, and then homogenized in an ice bath, followed by centrifugation at 6,000 rpm at 4 °C for 10 min. The collected supernatant was harvested, and the pH was measured a pH-320 acidity meter (Fangzhou Technology Co., Ltd.,

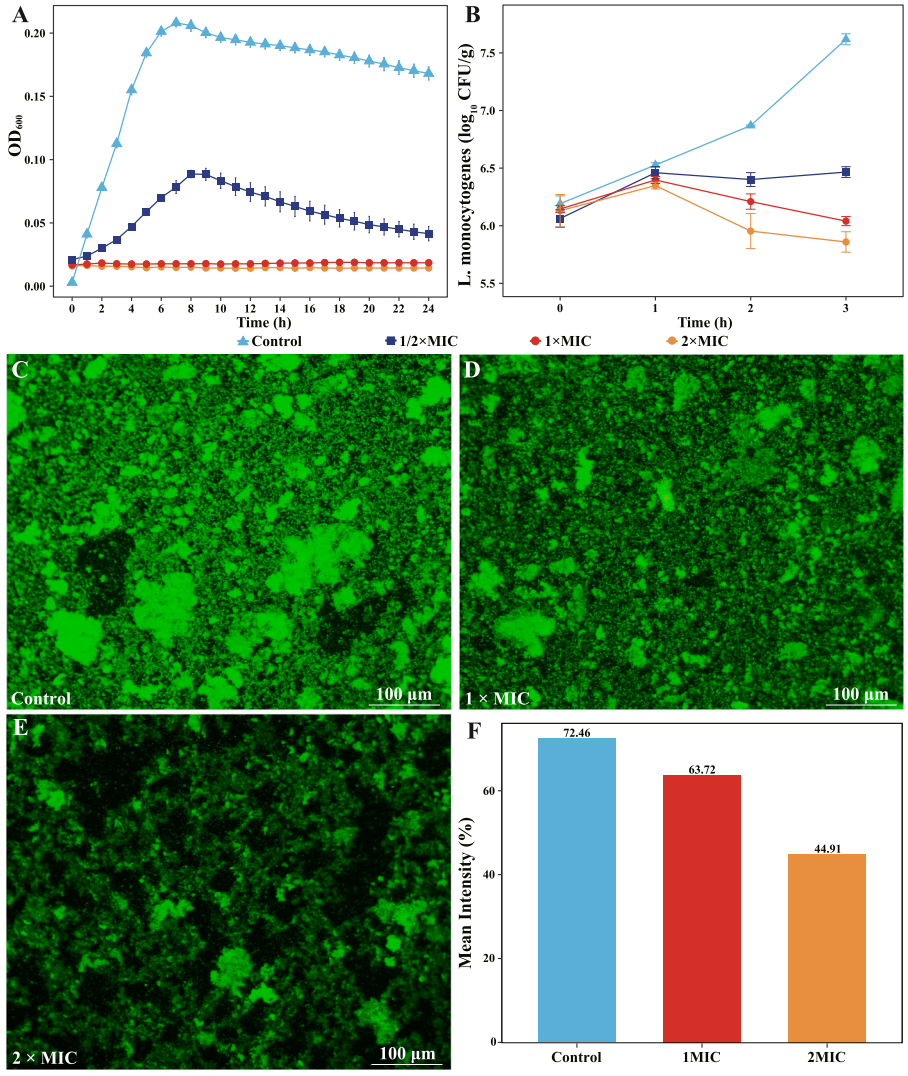

Fig. 1. Antimicrobial and anti-biofilm activity of the cell-free supernatant LCFS96 obtained from *Lactiplantibacillus plantarum* SHY96 against *Listeria monocytogenes*_02. (A) Growth curves of *L. monocytogenes*_02 in the control sample, and in the presence of LCFS96 at 1/2× MIC, 1× MIC, and 2× MIC. All OD values were presented after subtracting the blank sample. (B) Time-kill curve of *L. monocytogenes*_02 in the control sample, and in the presence of LCFS96 at 1/2× MIC, 1× MIC, and 2× MIC. Fluorescence microscopy observations of *L. monocytogenes*_02 biofilm formation without LCFS96 (C), and with LCFS96 at 1× MIC (D) and 2× MIC (E). Mean fluorescence intensity of *L. monocytogenes*_02 biofilm in the control sample, and treated with LCFS96 at 1× MIC and 2× MIC (F).

Chengdu, China). pH measurements were repeated three times for each sample.

2.6.4. Determination of total volatile basic nitrogen (TVB-N) content

TVB-N content in chicken breast samples was determined using the semi-micro-distillation method in accordance with the Chinese standard GB 5009.228–2016, as previously described by Ying et al. (2023). Briefly, 2 g of the treated meat sample was homogenized in 20 mL of deionized water and then filtered using a Whatman filter paper No. 1 (Whatman, Maidstone, England). Then, 5 mL of the filtrate was mixed with 5 mL of a 10 g/L magnesium oxide suspension in a Kjeldahl nitrogen distillation apparatus (Tianchang Kangpeng Experimental Equipment Co., Ltd., Anhui, China). Subsequently, volatile alkaline nitrogen was distilled into a receiving flask containing 10 mL of 20 g/L boric acid solution with five drops of a mixture of indicators, i.e., methyl red (1 g/mL) and methylene blue (1 g/mL) in a 2:1 (*v*/*v*) ratio. The mixed solution was distilled for 5 min, and then the boric acid absorbent was titrated with a standard titrant of 0.01 M sulfuric acid standard titrant. The volume of sulfuric acid consumed by the sample was denoted as V_1 (mL), while 5 mL of distilled water served as the control; V_2 (mL) indicated the volume of sulfuric acid consumed. TVB-N content was calculated using the appropriate formula:

$$X = \frac{(V_1 - V_2) \times 0.01 \times 14}{m \times 5/100}$$

2.6.5. Sensory evaluation

The experimental protocol was approved by the Institutional Review Board (College of Food Science, Southwest University), and panelists in the sensory experiments were informed of the experimental protocol and volunteered to participate. The panelists gave consent to take part in the experiment and to have their data used as part of the study.

Chicken breast samples were submitted to sensory evaluation to assess smell, color, texture, and acceptance, as previously described (Ying et al., 2023). Ten panelists were selected among graduate students enrolled at the College of Food Science, Southwest University, China, based on the following criteria: age between 20 and 28 years old and non-smokers. Samples were randomly labeled, then presented in a separate booth to each panelist for evaluation. A total of seven sensory evaluations were carried out on days 0, 2, 4, 6, 8, 10, and 12 throughout the experiment. Each panelist performed three different assays for each

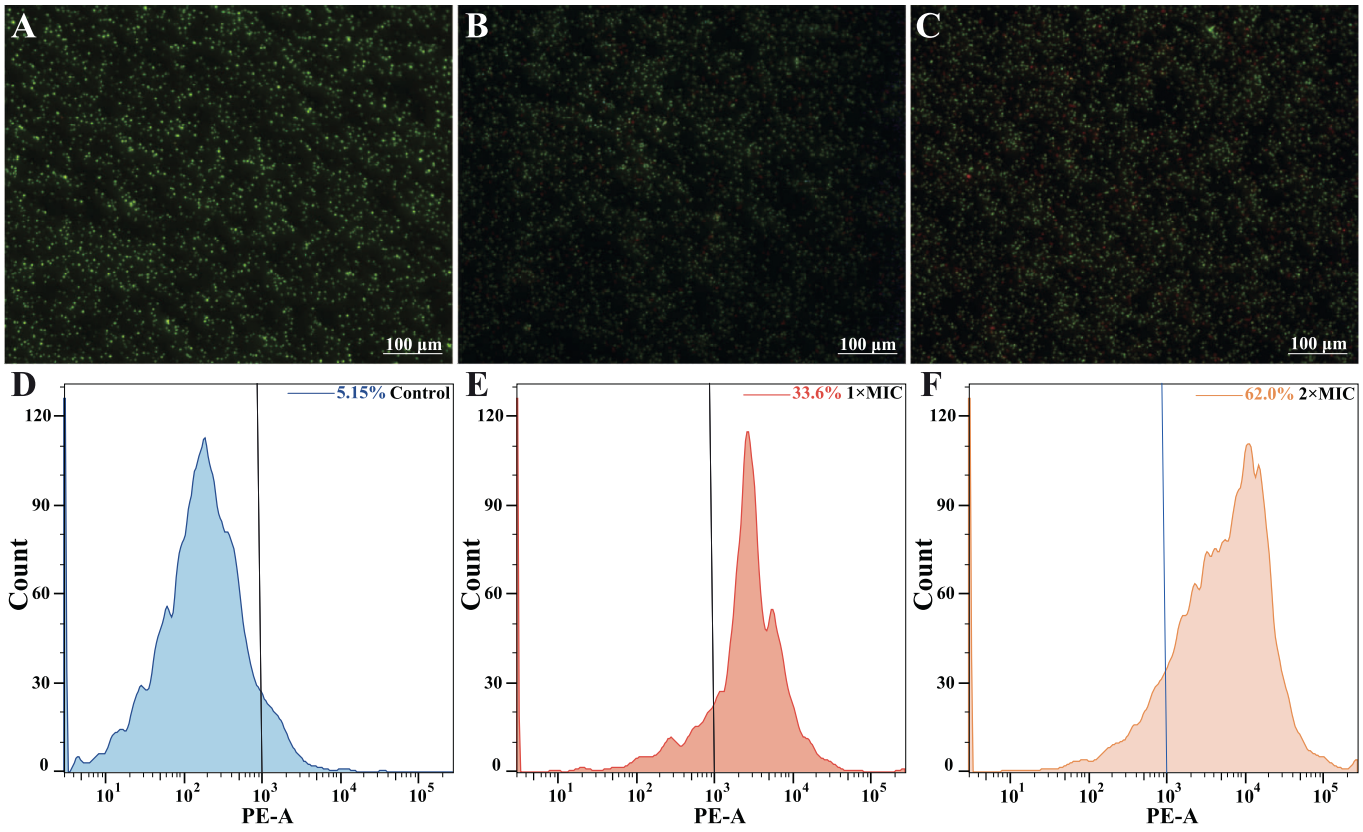

Fig. 2. Changes in metabolic activity of *Listeria monocytogenes*_02 cells treated the cell-free supernatant LCFS96 obtained from *Lactiplantibacillus plantarum* SHY96. Fluorescence microscopic observations of live green-stained *L. monocytogenes*_02 cells and red-stained dead cells in the control sample (no LCFS96) (A), and treated with LCFS96 at 1× MIC (B) and 2× MIC (C). Flow cytometry analysis of *L. monocytogenes*_02 cells in the control sample (D), and treated with LCFS96 at 1× MIC (E) and 2× MIC (F).

subsample. Sensory attributes were scored by panelists based on a 20-point scale (20 = liked very much, 18 = liked very much, 14 = liked generally, 12 = liked slightly, 10 = neither liked nor disliked, 8 = disliked slightly, 6 = disliked generally, 4 = disliked very much, and 2 = disliked very much). Samples with a score below 10 were considered unacceptable.

2.7. Statistical analysis

Data were expressed as mean values ± standard deviation and analyzed using SPSS statistics v.26.0 (SPSS Inc., Chicago, Illinois, USA). Analysis of variance (ANOVA) with Tukey's multiple comparison was used to compare sample groups, and differences were considered statistically significant when P values < 0.05.

3. Results

3.1. Antimicrobial effect of LCFS96 against L. monocytogenes_02

The MIC value for LCFS96 against *L. monocytogenes*_02 cells was 10 mg/mL. Compared to the control sample, the growth of *L. monocytogenes*_02 cells was significantly inhibited when treated with LCFS96 (Fig. 1A). Similar results are depicted in Fig. 1B, the number of *L. monocytogenes*_02 cells in the control group increased to 7.62 ± 0.05 $\log_{10}$ CFU/mL at 3 hpt. In contrast, a decrease in the number of *L. monocytogenes*_02 was observed after LCFS96 treatment at 3 hpt (1× MIC = 6.04 ± 0.04 $\log_{10}$ CFU/mL, 2× MIC = 5.86 ± 0.09 $\log_{10}$ CFU/mL). In addition, the biofilm formation ability of *L. monocytogenes*_02 was significantly impacted by LCFS96. Specifically, compared to control

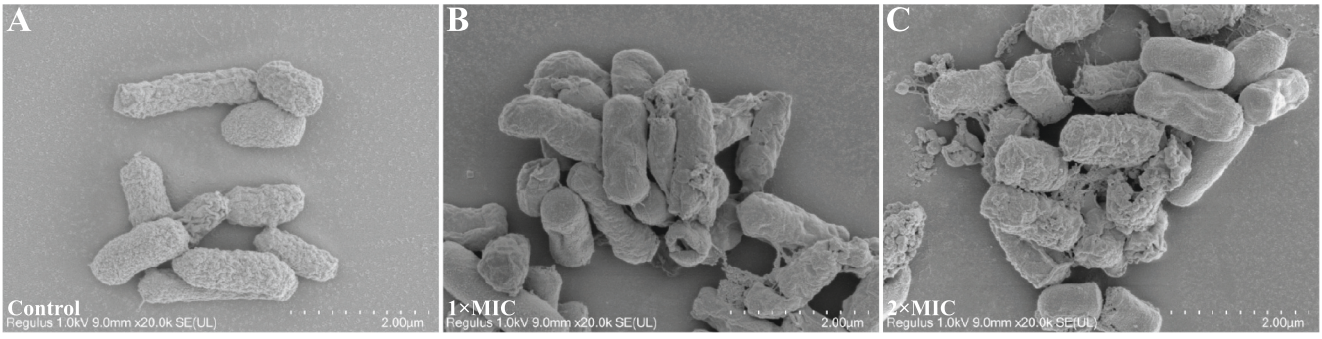

Fig. 3. SEM observations of *Listeria monocytogenes*_02 cells treated with the cell-free supernatant LCFS96 obtained from *Lactiplantibacillus plantarum* SHY96. (A) Untreated *L. monocytogenes*_02 cells, (B) cells treated with LCFS96 at 1× MIC, (C) cells treated with LCFS96 at 2× MIC.

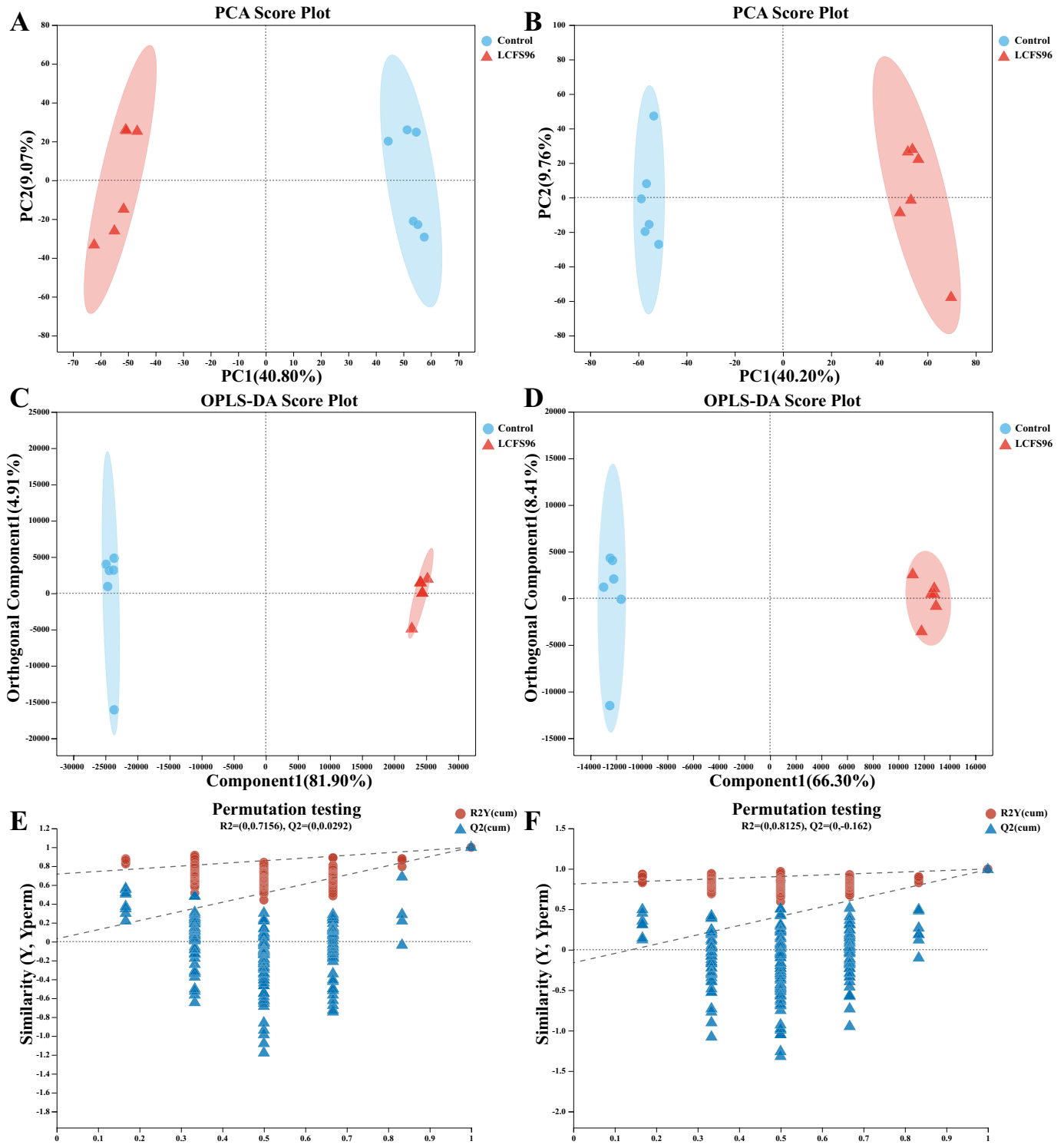

Fig. 4. Principal component analysis (PCA) score plots (A and B), orthogonal partial least-squares discriminant analysis (OPLS-DA) plots (C and D), and OPLS-DA permutation plot (E and F) of *Listeria monocytogenes*_02 cells untreated or treated with the cell-free supernatant LCFS96 obtained from *Lactiplantibacillus plantarum* SHY96 in ESI+ (A, C, and E) and ESI- (B, D, and F) modes.

samples (Fig. 1C), the density of *L. monocytogenes*_02 biofilms treated with LCFS96 at 1 × MIC (Fig. 1D) and 2 × MIC (Fig. 1E) was significantly reduced. Moreover, the results of mean fluorescence intensity revealed that biofilm density was significantly ($P < 0.01$) reduced to 87.94% and 61.98% when treated with LCFS96 at 1× MIC and 2× MIC, respectively, compared to control samples (Fig. 1F).

3.2. Impact of LCFS96 on *L. monocytogenes*_02 cell membrane integrity

*L. monocytogenes*_02 cells which were not treated with LCFS956 exhibited intense green fluorescence (Fig. 2A), which indicated a high proportion of viable cells. In contrast, *L. monocytogenes*_02 cells treated with LCFS96 at 1× MIC (Fig. 2B) and 2× MIC (Fig. 2C) showed a substantial increase in red fluorescence, which indicated the significant cell death occurred. Furthermore, flow cytometry quantitative results

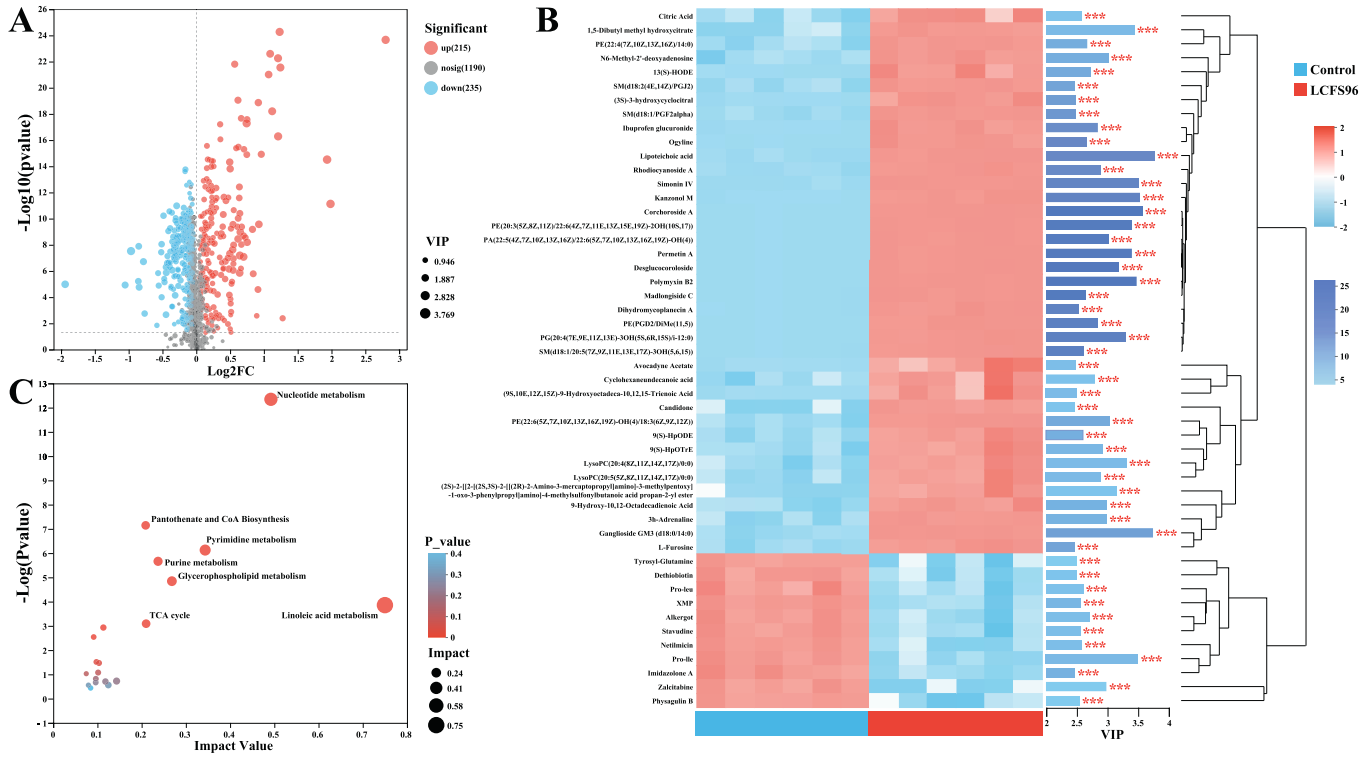

Fig. 5. Volcano plot of *Listeria monocytogenes*_02 metabolites in the control sample and in samples treated with the cell-free supernatant LCFS96 obtained from *Lactiplantibacillus plantarum* SHY96 (A). Heatmap hierarchical clustering analysis of the control sample and in samples treated with LCFS96 on *L. monocytogenes*_02 metabolites (B). Metabolic pathway analysis of *L. monocytogenes*_02 exposed to LCFS96 (C).

showed a significant increase in the proportion of red-stained *L. monocytogenes*_02 cells in samples treated with LCFS96 at 1× MIC (33.60%) (Fig. 2E) and 2× MIC (62.00%) (Fig. 2F) compared to the control sample (5.15%) (Fig. 2D) ($P < 0.05$).

3.3. Impact of LCFS96 on L. monocytogenes_02 morphology

SEM images revealed that untreated *L. monocytogenes*_02 cells maintained a uniform rod-shaped morphology with well-defined edges, clear outlines, and intact cell structures (Fig. 3A). In contrast, *L. monocytogenes*_02 cells treated with 1× MIC LCFS96 displayed subtle morphological changes, including surface roughening, shrinkage, and slight indentation (Fig. 3B). Importantly, intense morphological alterations were observed in *L. monocytogenes*_02 cells exposed to 2× MIC LCFS96, including marked collapse, deformation, and partial disintegration of the cell envelope (Fig. 3C).

3.4. Metabolomics analysis of L. monocytogenes

As shown in the PCA score plot (Fig. 4A and B), LCFS96-treated samples were clearly separated from the control group samples, thus indicating significant metabolic differences between the two groups. Similarly, OPLS-DA (Fig. 4C and D) further confirmed a clear separation in the metabolite profiles of the two sample groups. Specifically, R2X, R2Y, and Q2 values were 0.781, 0.997, and 0.995, respectively, thus indicating that the model has excellent fitting and predictive ability.

A total of 1640 metabolites were identified in both LCFS96-treated and control groups considering those with VIP > 1 and $P < 0.05$. Among these, 450 DAMs were found significantly altered, and visualization results are shown in the plotted volcano diagram (Fig. 5A), with the red color denoting significantly up-regulated metabolites, blue denoting significantly down-regulated metabolites, and grey denoting metabolites with differences that were not significant. In addition, 215 DAMs were up-regulated and 235 DAMs were down-regulated after LCFS96 treatment formed two distinct clusters (Fig. 5B), further indicating that the LCFS96 treatment significantly altered metabolic pathways in *L. monocytogenes*. Specifically, KEGG annotation results showed that DAMs were mainly involved in pathways related to linoleic acid metabolism, pyrimidine metabolism, purine metabolism, glycerophospholipid metabolism, pantothenate and CoA biosynthesis, and TCA cycle (Fig. 6).

3.5. Application of CFS to chicken breasts

3.5.1. Impact on microbiological contamination

Changes in the viable counts of *L. monocytogenes*_02 in chicken breast samples stored at 4 °C are shown in Fig. 7A. An increase in the viable counts of *L. monocytogenes*_02 was observed throughout the storage period in all treatment samples. On day 12, viable counts of *L. monocytogenes*_02 in control samples was 7.45 ± 0.09 $\log_{10}$ CFU/g, while in samples treated with LCFS96 at 1× MIC and 2× MIC were significantly lower, i.e., 6.63 ± 0.04 $\log_{10}$ CFU/g and 6.55 ± 0.04 $\log_{10}$ CFU/g, respectively.

3.5.2. Impact on pH

Changes in pH values in chicken breast samples are shown in Fig. 7B. In all samples, an initial decrease in pH was observed, followed by a subsequent increase. Notably, the rate in pH change in samples treated with 1× MIC and 2× MIC LCFS96 was consistently lower compared to control samples.

3.5.3. Impact on TVB-N content

TVB-N content in chicken breast samples during storage is shown in Fig. 7C. Throughout the storage period, an increase in TVB-N content was observed in all samples. Initially, TVB-N content in all samples was approximately 6.40 mg/100 g. On day 4, TVB-N content in control

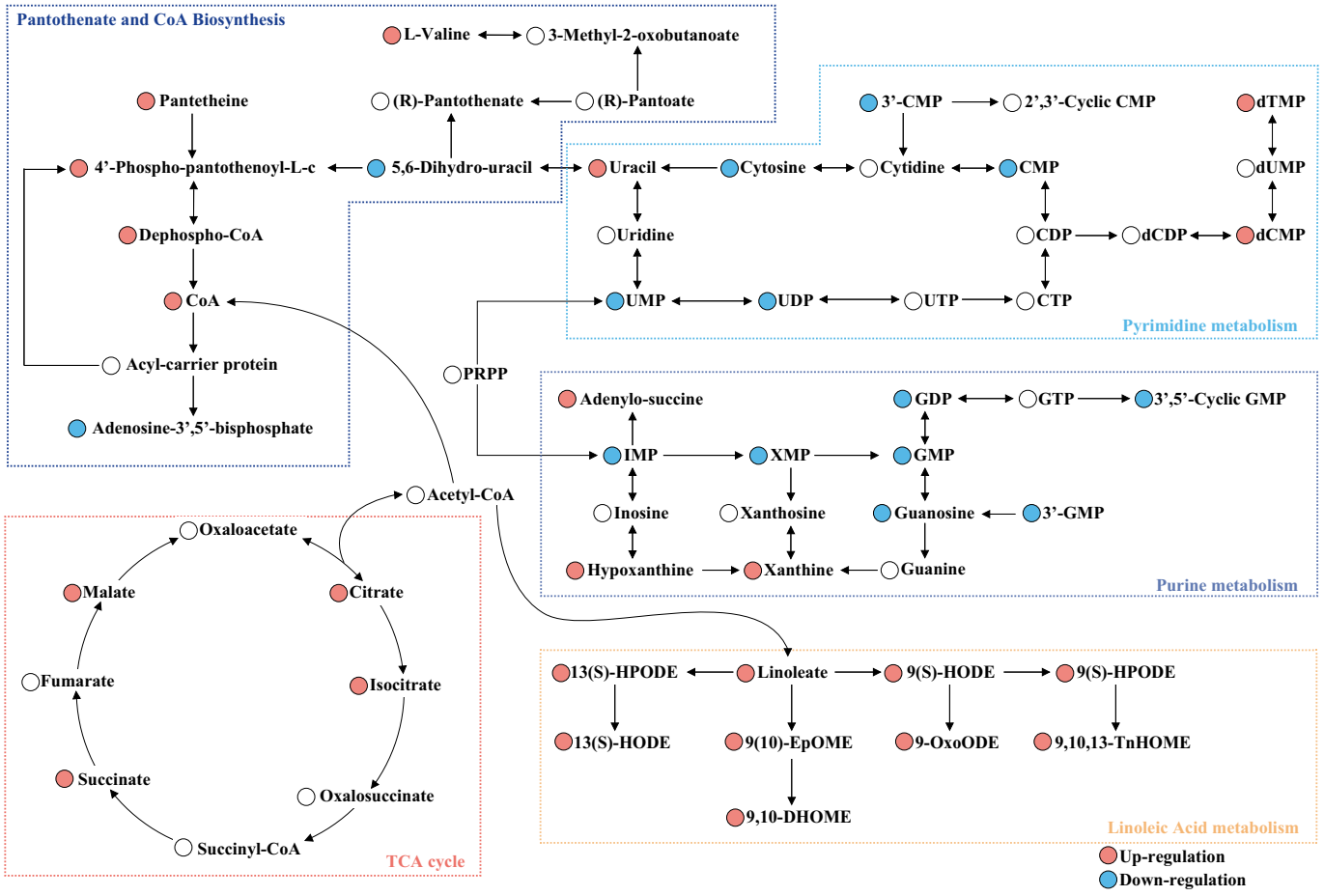

Fig. 6. Proposed schematic of metabolic alterations in *Listeria monocytogenes*_02 treated with the cell-free supernatant LCFS96 obtained from *Lactiplantibacillus plantarum* SHY96. Blue letters indicate significantly down-regulated metabolites, red letters indicate significantly up-regulated metabolites.

samples was found above the microbiological limit (16.85 ± 0.69 mg/100 g). In contrast, TVB-N content in samples treated with 1× MIC and 2× MIC LCFS96 increased more slowly; both were recorded at 9.14 ± 0.42 mg/100 g and 8.80 ± 0.49 mg/100 g at day 4, respectively. In addition, on day 12, TVB-N content in control samples considerably exceeded the microbiological limit (32.57 ± 0.50 mg/100 g), while samples treated with LCFS96 at 1× MIC and 2× MIC were closer to the upper microbiological limit, i.e., 16.66 ± 0.4 mg/100 g and 13.97 ± 0.45 mg/100 g.

3.5.4. Sensory evaluation

The results of the sensory evaluation of chicken breast samples are shown in Fig. 7D-G. Sourness and odor intensity in control samples gradually increased, with noticeable spoilage occurring after eight days of storage. However, the addition of LCFS96 at 1× MIC and 2× MIC led to significant delay at the onset of such undesirable sensory changes. Similarly, control samples exhibited a steady decline in sensory quality, culminating in a pronounced spoiled taste on day 12, while sensory deterioration in samples treated with LCFS96 at 1× MIC and 2× MIC occurred at a slower rate. Furthermore, minor but observable differences in color and texture in LCFS96-treated chicken breast samples compared to control samples by the end of the 12-day storage period.

4. Discussion

In the present study, the MIC value for LCFS96 against *L. monocytogenes*_02 cells was 10 mg/mL, which was similar to earlier findings. For instance, the MIC value for *L. plantarum* CFS against *Proteus mirabilis* was 12.5 mg/mL (Wang et al., 2021), whereas MIC values found for CFS obtained from *Lactobacillus* against *P. aeruginosa* were 62.5 μL/mL (Asadzadegan et al., 2023). Moreover, the growth of *L. monocytogenes*_02 cells was significantly decreased as a consequence of the exposure to LCFS96, with a dose-dependent effect on the degree of growth reduction. Specifically, the activity of *L. monocytogenes*_02 cells was significantly decreased when treated with LCFS96, and the growth of the cells was even lower under 1× MIC treatment compared with the control samples, with a gradual decrease in the viable count of *L. monocytogenes*_02 cells after 3 h of incubation. In addition, biofilm formation by *L. monocytogenes*_02 was significantly decreased when treated with LCFS96, suggesting that LCFS96 exhibits anti-biofilm activity against *L. monocytogenes*. Collectively, these results suggest that LCFS96 can effectively control cell growth and biofilm formation ability of *L. monocytogenes*_02, thus confirming the potential of LCFS96 as a natural antibacterial agent with promising application in the food industry.

LCFS96 exhibited an excellent antibacterial activity against *L. monocytogenes*_02. However, the mechanism underlying its antibacterial action is unclear. Herein, using fluorescence microscopy and flow cytometry, LCFS96 significantly reduced the viability of *L. monocytogenes*_02 cells. In particular, it was observed that *L. monocytogenes* cells had significantly reduced metabolic activity after LCFS96 treatment. This is consistent with findings from previous studies that the metabolic activity of *S. aureus*_26 and *E. coli*_02 cells decreased by 42.53% and 47.26%, respectively, after treatment with phytobactin LFX01 (Xin et al., 2023), whereas the metabolic activity of *E. coli* and *Salmonella Typhimurium* was found decreased by 30% and 31%, respectively, after treatment with bacteriocin (Kim et al., 2019). In addition, SEM analysis revealed the presence of surface wrinkles and

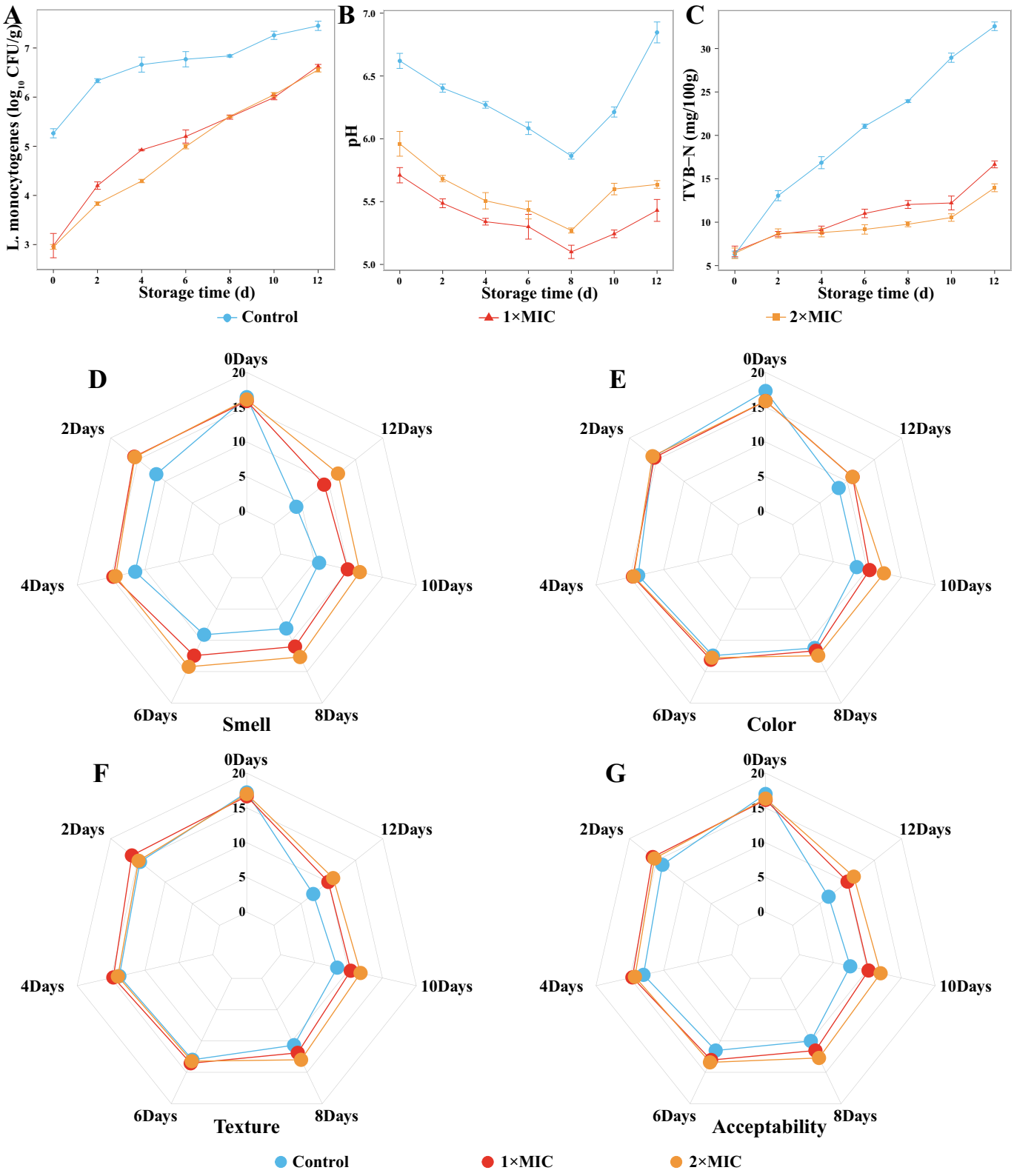

Fig. 7. Changes in the counts of *Listeria monocytogenes*_02 (A), pH (B), TVB-N (C) and sensory evaluation (D–G) of chicken breasts untreated or treated with the cell-free supernatant LCFS96 obtained from *Lactiplantibacillus plantarum* SHY96 during storage at 4 °C.

even ruptures on *L. monocytogenes*_02 cells following treatment with LCFS96, indicating that the treatment compromised the integrity of the cell membrane, potentially leading to increased membrane permeability. This is similar to findings reported for *Aeromonas hydrophila* ST3 treated with *L. plantarum* MY2 CFS (Wang et al., 2023). Therefore, our phenotypic results suggest that the inhibitory or killing effect of LCFS96 may be due to its ability to disrupt the membrane composition on *L. monocytogenes* cells, which likely results in the occurrence of molecular exchanges between the intracellular and extracellular environments, ultimately leading to changes in membrane potential and

biochemical metabolic activity.

Metabolomics is an important tool for resolving alterations in metabolite composition and metabolic function. Therefore, we focused on the metabolic and functional changes in *L. monocytogenes*_02 following treatment with LCFS96. It was found that LCFS96 treatment induced significant changes in metabolite profiles, mainly concentrated in linoleic acid metabolism, pyrimidine metabolism, purine metabolism, glycerophospholipid metabolism, pantothenate and CoA biosynthesis, and TCA cycle. These changes were also consistent with the observed phenotypic results. Moreover, it has been described that disturbances in pyrimidine and purine metabolism cause disruptions in DNA synthesis and metabolism, with deleterious effects on cellular repair and survival functions (Wang et al., 2023). After treatment with LCFS96, UMP, UDP, CMP, cytosine, as well as IMP, XMP, GMP, GDP, and guanosine were significantly down-regulated in *L. monocytogenes*; whereas uracil, hypoxanthine, and xanthine were significantly up-regulated, suggesting disturbances in pyrimidine metabolism and purine metabolism. This suggests that disturbed pyrimidine and purine metabolism induced by LCFS96 affects DNA repair, potentially leading to bacterial death, as previously reported (Cao et al., 2023). Furthermore, linoleic acid is involved in the construction of the phospholipid bilayer of the cell membrane, ensuring cell membrane permeability, thus being a key component of the cell structure. The increased levels of linoleic acid and its metabolites (including 9-oxo-ODE, 9,10-DHOME, and others) suggest that LCFS96 may have stimulated *L. monocytogenes* cells, resulting in enhanced linoleic acid metabolism, a finding similar to that reported by Xu et al. (2024). This result suggests that enhanced linoleic acid metabolism in *L. monocytogenes*_02 cells after LCFS treatment resulted in altered cell membrane permeability, which corresponds to the phenotypic observations (i.e., SEM). The TCA cycle is the main pathway providing cellular capacity, being associated with cell growth (Liu, Sun, et al., 2020). After treatment with LCFS96, the TCA cycle pathway of *L. monocytogenes*_02 was upregulated, and cellular metabolism was enhanced. It has been shown that antibacterial compounds can stimulate bacteria to undergo excessive metabolism, such as glucose metabolism and amino acid metabolism, leading to microbial dysfunction and death (Liang et al., 2024). Thus, we herein propose a tentative explanation for the antibacterial mechanism of LCFS96 against *L. monocytogenes* by combining phenotypic and metabolomics analyses. Specifically, when LCFS96 attacks *L. monocytogenes*, changes in structural substances (e.g., linoleic acid) on the cell membrane are observed, and subsequently altering biofilm structure and permeability. This causes intracellular substances to leak, and small molecules to enter the cell, thus changing osmotic pressure. Thereby, this leads to disturbances in purine and pyrimidine metabolism and a dramatic increase in energy metabolism. Thus, cell growth is inhibited, which may ultimately lead to cell death.

The preservative effect of natural antibacterial agents on meat is important for the development and future application of CFS-based antibacterial agents. Viable counts of *L. monocytogenes*, TVB-N content, and pH values were lower in CFS-treated sample groups compared to the control group. After 12 days of storage, *L. monocytogenes* counts decreased to approximately 14.88% and 12.56% in samples treated with LCFS96 at 1× MIC and 2× MIC, respectively, compared to the control sample. Moreover, TVB-N content in treated chicken breasts was significantly lower compared to the control group at 4 °C for 12 days of storage, which was consistent with the bacterial counts results. Moreover, LCFS96 inhibited the growth of *L. monocytogenes*_02 and slowed down protein breakdown in chicken breasts, which in alignment with the results of the application of the natural antimicrobial agent of *Lactobacillus paracasei* FX-6 to chicken breasts during storage under refrigeration (Duan et al., 2020). In addition, the pH of chicken breasts contaminated with *L. monocytogenes*_02 showed a downward and then an upward trend over a 12-day period, which may be attributed to the oxidation of unsaturated fatty acids to produce lactic acid and inorganic phosphate, and the growth of *L. monocytogenes* accelerated the spoilage of chicken breasts. This resulted in a decrease in pH initially (Zhu et al., 2023), followed by an increase due to protein degradation and the production of alkaline compounds (Dong et al., 2024). Such changes in pH values are in agreement with the study of Q. Li et al. (2024).

Sensory assessment is the most intuitive way to determine the deterioration in the quality of meat products. For instance, deterioration of fresh chicken meat results in sticky surface and the production of an unpleasant odor (Ma et al., 2022). In addition, deterioration of fresh pork tenderloin results in oxidization of lipids and proteins, as well as production of ammonia, amines, aldehydes, and ketones, thus releasing an unpleasant odor (Hu et al., 2022). Herein, sensory evaluation analysis showed that treatment with LCFS96 maintained the organoleptic properties of chicken breast meat, especially odor, which is consistent with previously reported findings on chicken treated with protocatechualdehyde and linalool (He et al., 2023; Liao et al., 2023). Taken together, our findings revealed that LCFS96 effectively inhibited the growth of a foodborne pathogen for at least 12 days of storage, slowed down nutrient loss, and maintained sensory properties in a chicken breast model developed herein, suggesting that it could be a promising preservative for potential application in chicken breast meat.

5. Conclusion

In this study, LCFS96 exhibited potent antibacterial and anti-biofilm activity against *L. monocytogenes*_02. Its antimicrobial effect was primarily attributed to disruption of cellular metabolism and membrane integrity. Metabolomic analysis identified key metabolic pathways affected, including linoleic acid metabolism, pyrimidine and purine metabolism, glycerophospholipid metabolism, pantothenate and CoA biosynthesis, and the TCA cycle. In addition, LCFS96 inhibited the growth of *L. monocytogenes*_02 in chicken breast meat. It reduced protein degradation and maintained sensory quality during storage for up to 12 days. This indicates that LCFS96 was a promising natural preservative. Compared to traditional preservatives that rely on broad-spectrum antimicrobial action, LCFS96 targets metabolic pathways and membrane integrity for potent antimicrobial and anti-biofilm effects. It has a unique biochemical mechanism and advantages over conventional preservatives and shows potential in food preservation. LCFS96 can be an important tool to improve food safety and extend shelf life in a healthy and sustainable way.

CRediT authorship contribution statement

Ming Liang: Writing – review & editing, Writing – original draft, Investigation, Data curation, Conceptualization. **Hongwei Wang:** Writing – review & editing, Resources. **Zhaoquan Zhou:** Investigation. **Yechuan Huang:** Resources, Conceptualization. **Huayi Suo:** Resources, Methodology, Conceptualization.

Declaration of competing interest

The authors declare that they have no known competing financial interests or personal relationships that could have appeared to influence the work reported in this paper.

Acknowledgements

This study was supported by the Sichuan Science and Technology Program (2023YFS0399), the Major Science and Technology Special Projects in the Tibet Autonomous Region (XZ202201ZD0001N), Chongqing Modem Agricultural Industry Technology System (CQMAITS202314), the key science and technology project of Jingmen city (2022YFZD058), and Joint Graduate Students of Jingchu Polytechnic University Research Fund (YBYJS2405). We would like to thank MogoEdit (https://www.mogoedit.com) for its English editing during the preparation of this manuscript.

Appendix A. Supplementary data

Supplementary data to this article can be found online at https://doi.org/10.1016/j.fochx.2024.102078.

Data availability

Data will be made available on request.

References

Asadzadegan, R., Haratian, N., Sadeghi, M., Maroufizadeh, S., Mobayen, M., Sedigh Ebrahim Saraei, H., & Hasannejad-Bibalan, M. (2023). Antibiofilm and antimicrobial activity of *Lactobacillus* cell free supernatant against *Pseudomonas aeruginosa* isolated from burn wounds. *International Wound Journal, 20*(10), 4112–4121. https://doi.org/10.1111/iwj.14305

Bodie, A. R., O'Bryan, C. A., Olson, E. G., & Ricke, S. C. (2023). Natural antimicrobials for *Listeria monocytogenes* in ready-to-eat meats: Current challenges and future prospects. *Microorganisms, 11*(5), 1301. https://doi.org/10.3390/microorganisms11051301

Cao, S., Wang, J., You, X., Zhou, B., Wang, Y., & Zhou, Z. (2023). Purine metabolism and pyrimidine metabolism alteration is a potential mechanism of BDE-47-induced apoptosis in marine rotifer *Brachionus plicatilis*. *International Journal of Molecular Sciences, 24*(16), 12726. https://doi.org/10.3390/ijms241612726

Dejene, F., Regasa Dadi, B., & Tadesse, D. (2021). In vitro antagonistic effect of lactic acid bacteria isolated from fermented beverage and finfish on pathogenic and foodborne pathogenic microorganism in Ethiopia. *International Journal of Microbiology, 2021*, 1–10. https://doi.org/10.1155/2021/5370556

Dong, M., Liang, F., Cui, S., Mao, B.-B., Huang, X.-H., & Qin, L. (2024). Insights into the effects of steaming on organoleptic quality of salmon (*Salmo salar*) integrating multi-omics analysis and electronic sensory system. *Food Chemistry, 434*, Article 137372. https://doi.org/10.1016/j.foodchem.2023.137372

Duan, X., Duan, S., Wang, Q., Ji, R., Cao, Y., & Miao, J. (2020). Effects of the natural antimicrobial substance from *Lactobacillus paracasei* FX-6 on shelf life and microbial composition in chicken breast during refrigerated storage. *Food Control, 109*, Article 106906. https://doi.org/10.1016/j.foodcont.2019.106906

European Food Safety Authority & European Centre for Disease Prevention and Control. (2022). The European Union one health 2021 zoonoses report. *EFSA Journal, 20*(12). https://doi.org/10.2903/j.efsa.2022.7666

FAO and WHO. (2022). *isteria monocytogenes* in ready-to-eat (RTE) foods: attribution, characterization and monitoring – Meeting report. *Microbiological Risk Assessment Series No. 38*. 10.4060/cc2400en.

He, R., Chen, W., Chen, H., Zhong, Q., Zhang, H., Zhang, M., et al. (2022). Antibacterial mechanism of linalool against *L. monocytogenes*, a metabolomic study. *Food Control, 132*, Article 108533. https://doi.org/10.1016/j.foodcont.2021.108533

He, R., Zhong, Q., Chen, W., Zhang, M., Pei, J., Chen, H., et al. (2023). Transcriptomic and proteomic investigation of metabolic disruption in *Listeria monocytogenes* triggered by linalool and its application in chicken breast preservation. *LWT - Food Science and Technology, 176*, Article 114492. https://doi.org/10.1016/j.lwt.2023.114492

Hu, H., Yong, H., Zong, S., Jin, C., & Liu, J. (2022). Effect of chitosan/starch aldehyde-catechin conjugate composite coating on the quality and shelf life of fresh pork loins. *Journal of the Science of Food and Agriculture, 102*(12), 5238–5249. https://doi.org/10.1002/jsfa.11877

Jamshidi, A., & Zeinali, T. (2019). Significance and characteristics of *Listeria monocytogenes* in poultry products. *International Journal of Food Science, 2019*, 1–7. https://doi.org/10.1155/2019/7835253

Jiang, Y. H., Xin, W. G., Yang, L. Y., Ying, J. P., Zhao, Z. S., Lin, L. B., et al. (2022). A novel bacteriocin against *Staphylococcus aureus* from *Lactobacillus paracasei* isolated from Yunnan traditional fermented yogurt: Purification, antibacterial characterization, and antibiofilm activity. *Journal of Dairy Science, 105*(3), 2094–2107. https://doi.org/10.3168/jds.2021-21126

Jiang, Y. H., Xin, W.-G., Zhang, Q.-L., Lin, L.-B., & Deng, X.-Y. (2022). A novel bacteriocin against *Shigella flexneri* from *Lactiplantibacillus plantarum* isolated from tilapia intestine: Purification, antibacterial properties and antibiofilm activity. *Frontiers in Microbiology, 12*, Article 779315. https://doi.org/10.3389/fmicb.2021.779315

Khan, F. M., Chen, J.-H., Zhang, R., & Liu, B. (2023). A comprehensive review of the applications of bacteriophage-derived endolysins for foodborne bacterial pathogens and food safety: Recent advances, challenges, and future perspective. *Frontiers in Microbiology, 14*, 1259210. https://doi.org/10.3389/fmicb.2023.1259210

Kim, S. H., Kim, W. J., & Kang, S.-S. (2019). Inhibitory effect of bacteriocin-producing *Lactobacillus brevis* DF01 and *Pediococcus acidilactici* K10 isolated from kimchi on enteropathogenic bacterial adhesion. *Food Bioscience, 30*, Article 100425. https://doi.org/10.1016/j.fbio.2019.100425

Li, Q., Wang, B., Peng, S., Wei, H., Li, P., Leng, Y., et al. (2024). Photodynamic inactivation of *Listeria monocytogenes* using a natural aggregation-induced emission photosensitizer and its application in salmon preservation. *LWT - Food Science and Technology, 193*, Article 115762. https://doi.org/10.1016/j.lwt.2024.115762

Liang, T., Wang, X., Chen, L., Ding, L., Wu, J., Zhang, J., et al. (2024). Transcriptomic and metabolomic analyses reveal the antibacterial mechanism of *Zanthoxylum bungeanum Maxim*. Essential oil against GBS. *Food Bioscience, 57*, Article 103528. https://doi.org/10.1016/j.fbio.2023.103528

Liao, S., Tian, L., Qi, Q., Hu, L., Wang, M., Gao, C., et al. (2023). Transcriptome analysis of protocatechualdehyde against *Listeria monocytogenes* and its effect on chicken quality characteristics. *Foods, 12*(13). https://doi.org/10.3390/foods12132625. Article 13.

Liu, H., Liu, W., He, X., Chen, X., Yang, J., Wang, Y., Li, Y., et al. (2020). Characterization of a cell density-dependent sRNA, Qrr, and its roles in the regulation of the quorum sensing and metabolism in *Vibrio alginolyticus*. *Applied Microbiology and Biotechnology, 104*(4), 1707–1720. https://doi.org/10.1007/s00253-019-10278-3

Liu, Y., Sun, W., Sun, T., Gorris, L. G. M., Wang, X., Liu, B., et al. (2020). The prevalence of *Listeria monocytogenes* in meat products in China: A systematic literature review and novel meta-analysis approach. *International Journal of Food Microbiology, 312*, Article 108358. https://doi.org/10.1016/j.ijfoodmicro.2019.108358

Luo, L., Yi, L., Chen, J., Liu, B., & Lü, X. (2021). Antibacterial mechanisms of bacteriocin BM1157 against *Escherichia coli* and *Cronobacter sakazakii*. *Food Control, 123*, Article 107730. https://doi.org/10.1016/j.foodcont.2020.107730

Ma, M., Zhao, J., Yan, X., Zeng, Z., Wan, D., Yu, P., et al. (2022). Synergistic effects of monocaprin and carvacrol against *Escherichia coli* O157:H7 and *Salmonella* Typhimurium in chicken meat preservation. *Food Control, 132*, Article 108480. https://doi.org/10.1016/j.foodcont.2021.108480

Ma, M., Zhao, J., Zeng, Z., Yu, P., Xia, J., Wan, D., et al. (2023). Deciphering the antibacterial mechanism of monocaprin against methicillin-resistant *Staphylococcus aureus* by integrated transcriptomic and metabolomic analyses and its application in pork preservation. *LWT - Food Science and Technology, 177*, Article 114569. https://doi.org/10.1016/j.lwt.2023.114569

Marmion, M., Macori, G., Ferone, M., Whyte, P., & Scannell, A. G. M. (2022). Survive and thrive: Control mechanisms that facilitate bacterial adaptation to survive manufacturing-related stress. *International Journal of Food Microbiology, 368*, Article 109612. https://doi.org/10.1016/j.ijfoodmicro.2022.109612

Palma, F., Brauge, T., Radomski, N., Mallet, L., Felten, A., Mistou, M. Y., et al. (2020). Dynamics of mobile genetic elements of *Listeria monocytogenes* persisting in ready-to-eat seafood processing plants in France. *BMC Genomics, 21*(1), 130. https://doi.org/10.1186/s12864-020-6544-x

Qian, C., Jin, L., Zhu, L., Zhou, Y., Chen, J., Yang, D., et al. (2022). Metabolomics-driven exploration of the antibacterial activity and mechanism of 2-Methoxycinnamaldehyde. *Frontiers in Microbiology, 13*. https://doi.org/10.3389/fmicb.2022.864246

Silva, D. R., de Sardi, J. C. O., de Pitangui, N. S., Roque, S. M., da Silva, A. C. B., & Rosalen, P. L. (2020). Probiotics as an alternative antimicrobial therapy: Current reality and future directions. *Journal of Functional Foods, 73*, Article 104080. https://doi.org/10.1016/j.jff.2020.104080

Toushik, S. H., Kim, K., Ashrafudoulla, M., Mizan, M. F. R., Roy, P. K., Nahar, S., et al. (2021). Korean kimchi-derived lactic acid bacteria inhibit foodborne pathogenic biofilm growth on seafood and food processing surface materials. *Food Control, 129*, Article 108276. https://doi.org/10.1016/j.foodcont.2021.108276

Wang, D., Liu, Y., Li, X., Chen, S., Deng, J., Li, C., … Wei, Y. (2023). Unraveling the antibacterial mechanism of *Lactiplantibacillus plantarum* MY2 cell-free supernatants against *Aeromonas hydrophila* ST3 and potential application in raw tuna. *Food Control, 145*, 109512. https://doi.org/10.1016/j.foodcont.2022.109512

Wang, Y., Pei, H., Liu, Y., Huang, X., Deng, L., Lan, Q., et al. (2021). Inhibitory mechanism of cell-free supernatants of *Lactiplantibacillus plantarum* on *Proteus mirabilis* and influence of the expression of histamine synthesis-related genes. *Food Control, 125*, Article 107982. https://doi.org/10.1016/j.foodcont.2021.107982

Xin, W. G., Wu, G., Ying, J. P., Xiang, Y. Z., Jiang, Y. H., Deng, X. Y., et al. (2023). Antibacterial activity and mechanism of action of bacteriocin LFX01 against *Staphylococcus aureus* and *Escherichia coli* and its application on pork model. *Meat Science, 196*, Article 109045. https://doi.org/10.1016/j.meatsci.2022.109045

Xu, J. C., Chen, Z. Y., Huang, X. J., Wu, J., Huang, H., Niu, L. F., et al. (2024). Multi-omics analysis reveals that linoleic acid metabolism is associated with variations of trained immunity induced by distinct BCG strains. Science. *Advances, 10*(14), eadk8093. https://doi.org/10.1126/sciadv.adk8093

Yilmaz, B., Bangar, S. P., Echegaray, N., Suri, S., Tomasevic, I., Manuel Lorenzo, J., et al. (2022). The impacts of *Lactiplantibacillus plantarum* on the functional properties of fermented foods: A review of current knowledge. *Microorganisms, 10*(4), 826. https://doi.org/10.3390/microorganisms10040826

Ying, J. P., Wu, G., Zhang, Y. M., & Zhang, Q. L. (2023). Proteomic analysis of *Staphylococcus aureus* exposed to bacteriocin XJS01 and its bio-preservative effect on raw pork loins. *Meat Science, 204*, Article 109258. https://doi.org/10.1016/j.meatsci.2023.109258

Yuan, L., Feng, W., Zhang, Z., Peng, Y., Xiao, Y., & Chen, J. (2021). Effect of potato starch-based antibacterial composite films with thyme oil microemulsion or microcapsule on shelf life of chilled meat. *LWT - Food Science and Technology, 139*, Article 110462. https://doi.org/10.1016/j.lwt.2020.110462

Zhang, H. Y., Zuo, X. Y., Sun, B. Y., Wei, B. Q., Fu, J. J., & Xiao, X. Q. (2023). Fuzzy-PID-based atmosphere packaging gas distribution system for fresh food. *Applied Sciences, 13*(4), 2674. https://doi.org/10.3390/app13042674

Zhang, R. H., Chen, X. J., Wan, Z. Z., Wang, M., & Xiao, X. Q. (2023). Deep learning-based oyster packaging system. *Applied Sciences, 13*(24), 13105. https://doi.org/10.3390/app132413105

Zhao, Y., Ren, J., Jiang, H., Chen, X., Xu, M., Li, Y., et al. (2021). Metabolomics and lipidomics analyses delineating Hfq deletion- induced metabolic alterations in *Vibrio alginolyticus*. *Aquaculture, 535*, Article 736349. https://doi.org/10.1016/j.aquaculture.2021.736349

Zhu, X., Yan, H., Cui, Z., Li, H., Zhou, W., Liu, Z., et al. (2023). Ultrasound-assisted blue light killing *Vibrio parahaemolyticus* to improve salmon preservation. *Ultrasonics Sonochemistry, 95*, Article 106389. https://doi.org/10.1016/j.ultsonch.2023.106389